International Journal of Fracture **98:** 225–241, 1999.

Snap-back analysis of fracture evolution in multi-cracked solids using boundary element method

ALBERTO CARPINTERI and ILARIA MONETTO
Department of Structural Engineering, Politecnico di Torino, Corso Duca degli Abruzzi 24, 10129 Torino, Italy
e-mail: carpinteri@polito.it

Received 1 December 1997; accepted in revised form 11 August 1998

Abstract. According to the Linear Elastic Fracture Mechanics criteria, a numerical model is developed to simulate the failure evolution of multi-cracked finite plates by means of an incremental loading procedure. A modified crack length control scheme is used in order to analyse such problems depending on one or more independent parameters. The aim is to provide information about a discontinuous response, such as the snap-back instability, which can be highlighted only by a deformation controlled process. The load vs. displacement curve, included possible snap-back branches, is numerically traced by means of a procedure based on the Displacement Discontinuity Boundary Element Method. With reference to finite plates with ordered crack distributions in plane strain loading conditions, the model is applied in order to analyse the effects of the crack interaction on the fracture evolution.

Key words: Snap-back instability, crack length control scheme, fracture evolution, multi-cracked solid.

1. Introduction

Cracked solids often present an unstable structural behaviour which is represented by a negative slope of the load vs. displacement softening branch. This means that only the load must decrease to obtain slow and stable crack propagation. On the other hand, the global behaviour can range from ductile to brittle, in dependence on material properties, structure geometry and loading conditions. For extremely brittle cases crack propagation occurs suddenly with a catastrophic drop in the load carrying capacity and the load vs. displacement softening branch assumes a positive slope. If the loading process is displacement controlled, the load vs. displacement curve presents a discontinuity and the representative point drops onto the lower branch with negative slope. This means that both load and displacement must decrease to obtain a controlled crack extension.

Such a phenomenon, the so called *snap-back instability*, was first described in the framework of Structural Mechanics with reference to the buckling analysis of thin cylindrical shells under axial compression (Karman and Tsien, 1941). Usually post-critical equilibrium states are not taken into account in the design of a structure; nevertheless, the prediction of the overall response can be of great convenience. From this point of view, snap-through and snap-back buckling phenomena (Figure 1) are some of the most difficult problems in nonlinear structural analysis. According to the Finite Element Method (FEM), the nonlinear solution is based on an incremental iterative procedure that can fail depending on the adopted control scheme. If the system is controlled by the load, both the dynamic snapping phenomena can result and the possible descending post-limit response cannot be traced. On the other hand, if a single displacement component is selected as a controlling parameter, whereas the corresponding load level is taken as unknown, the response related to the snap-back instabilities continues

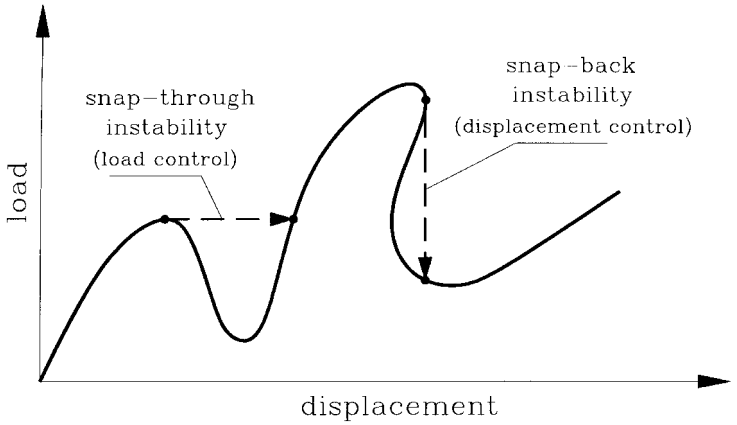

Figure 1. Dynamic snapping phenomena.

to be virtual. In order to overcome these problems and to compute post-critical equilibrium states, several strategies have been proposed (Ramm, 1981). Wempner (1971), Riks (1978) and Crisfield (1981) in their *arc-length control scheme* use the length of the equilibrium path as loading parameter, adding an auxiliary equation in the set governing the equilibrium of the structure. This method is the most advantageous in the entire loading process, being successful in both snap-through and snap-back buckling problems.

Only later on the snap-back phenomenon has been proved to be characteristic of some Fracture Mechanics problems (Carpinteri, 1985). In the framework of Linear Elastic Fracture Mechanics (LEFM) it tends to reproduce the classical Griffith instability for extremely brittle systems, depending on material properties and structure geometry.

With reference to a cracked homogeneous solid, the snap-back instability develops only if both load and displacement decrease. The related branch may be captured only if the loading process is controlled by a function always monotonically increasing after the maximum load is reached. In the specific case of a fracture evolution analysis, such a monotonically increasing function can coincide with the crack mouth opening or sliding displacement as well as with the crack length. Based on such considerations, other control schemes have been proposed and proved to be more suitable in Fracture Mechanics problems. For instance, the *indirect displacement control scheme* developed by Rots and de Borst (1987) refers to the crack mouth sliding displacement (CMSD) as driving parameter. This technique differs from the standard arc-length method in that it involves a constraint equation based on a few dominant displacement parameters, such as the crack mouth opening or sliding displacement, rather than on a global norm of displacement increments, such as the length of the equilibrium path. On the other hand, the *crack length control scheme* uses the crack length itself in Mode I (Carpinteri et al., 1986; Carpinteri and Fanelli, 1987; Bocca et al., 1989; Carpinteri, 1989; Carpinteri and Colombo, 1989; Saleh and Aliabadi, 1995) as well as in Mixed Mode (Carpinteri and Valente, 1988; Bocca et al., 1990; Saleh and Aliabadi, 1995; Barpi and Valente, 1998) loading conditions.

Using the FEM, several simulations of brittle failure behaviour in homogeneous finite plates have been carried out under CMSD or crack length control. Single and double edge notched specimens have been mainly considered for the three point bending test (Carpinteri, 1985; Carpinteri et al., 1986; Carpinteri and Fanelli, 1987; Bocca et al., 1989; Carpinteri, 1989; Carpinteri and Colombo, 1989) and for the four point shear test (Rots and de Borst,

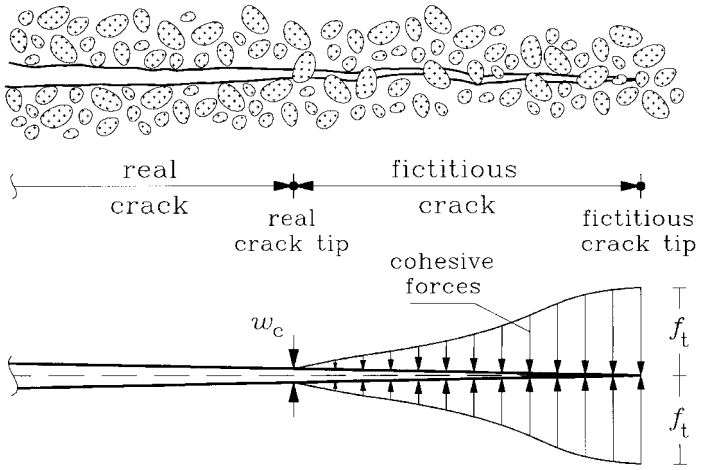

Figure 2. The fictitious crack model.

1987; Carpinteri and Valente, 1988; Bocca et al., 1990; Barpi and Valente, 1998). In both cases the problem is driven by one independent parameter: the crack mouth sliding displacement or the crack length, which is the same for both cracks in double edge notched specimens due to symmetry. On the other hand, if multi-cracked plates are considered, where a crack distribution is thought of as embedded in an elastic matrix, the length of a generic crack is not a strictly monotonic increasing function. Due to the elastic crack interaction, the extension of a specific crack can be arrested and, at the same time, another crack may grow. It follows that the crack controlling the fracture evolution can change at each step of the loading process.

This paper describes a modification of the crack length control scheme to analyse the fracture mechanics of solids containing a distribution of interacting cracks. By means of a procedure based on the Boundary Element Method (BEM), a numerical model for crack growth is developed according to the LEFM criteria. A slow and controlled crack propagation is obtained increasing the crack lengths in an incremental loading process. With reference to finite plates with one or more rows of evenly spaced collinear cracks in plane strain conditions, some illustrative problems are shown. The snap-back branches of the load vs. displacement curve are numerically captured and the effects of the crack interaction on fracture evolution are analysed.

2. Crack length control scheme

The crack length control scheme was first used to model cohesive crack propagation in a concrete-like material (Carpinteri, 1985). According to the *fictitious crack model* proposed by Hillerborg, Modeer and Petersson (1976), the nonlinear and dissipative phenomena occurring at the crack tip can be described by a process zone in front of the real crack tip, with cohesive forces representing the aggregate interlocking and bridging (Figure 2). The intensity of these forces depends on the opening w of the fictitious crack, according to the $\sigma - w$ cohesive law of the material. The real crack tip coincides with the point where the distance between the crack faces is equal to the critical value w_c of the crack opening displacement and the normal stress vanishes. On the other hand, the fictitious crack tip is defined as the point where the normal stress attains the maximum value f_t and the crack opening vanishes.

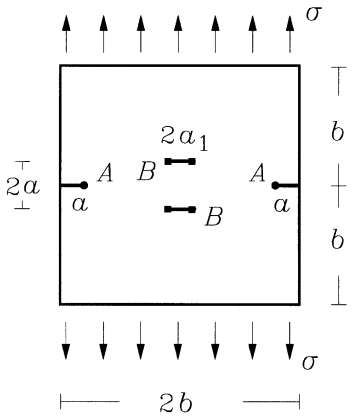

Figure 3. Square plate in tension with two edge cracks and two central cracks.

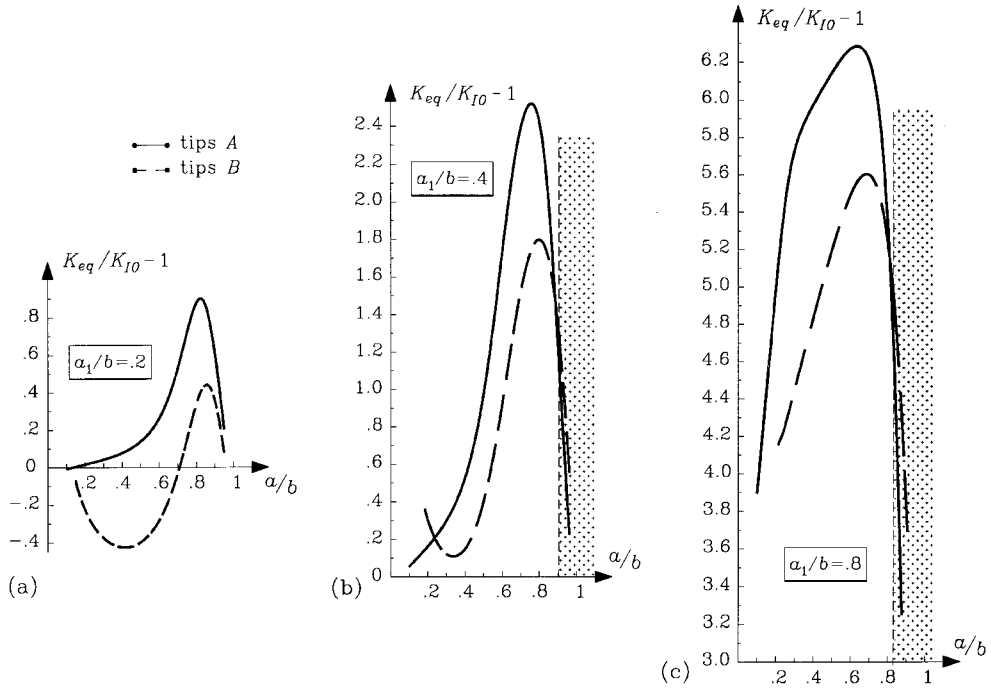

Figure 4. SIFs at the crack tips of the finite plate of Figure 3: (a) $a_1/b = 0.2$; (b) $a_1/b = 0.4$; (c) $a_1/b = 0.8$.

A numerical FEM procedure was implemented to simulate a loading process where the fictitious crack depth is the parameter incremented step by step (Carpinteri, 1985). Real crack depth, external load and deflection were obtained at each step after an iterative computation. With reference to the three point bending test or to the four point shear test geometry, numerical simulations of Mode I as well as Mixed Mode cohesive crack propagation were presented in (Carpinteri et al., 1986; Carpinteri and Fanelli, 1987; Carpinteri and Valente, 1988; Bocca et al., 1989; Carpinteri, 1989; Carpinteri and Colombo, 1989; Bocca et al., 1990; Barpi and Valente, 1998). Another successful approach is developed in (Saleh and Aliabadi, 1995), where the Dual Boundary Element Method (DBEM) is shown to be computationally

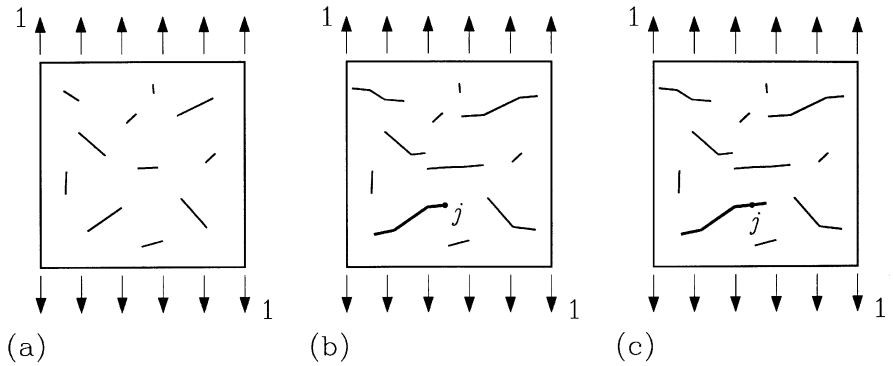

Figure 5. Fracture evolution in a multi-cracked plate: (a) initial geometry; (b) the ith generic loading step and (c) the subsequent $i + 1$th step.

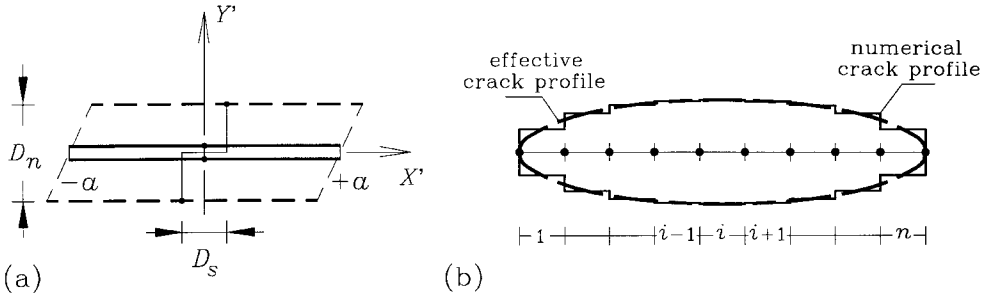

Figure 6. DDBEM: (a) a single displacement discontinuity element; (b) discretization of a crack with n boundary elements.

effective in simulating the nonlinear behaviour of cracking in concrete and to obtain results in good agreement with the cited FEM analyses.

On the other hand, the crack length control scheme is useful to model brittle crack propagation even when the nonlinear and dissipative phenomena occurring at the crack tip are negligible. Assigned the geometry and a unit load distribution, an evaluation $\overline{K}_{\text{eq}}$ of the equivalent SIF at the crack tip can be obtained; although exact closed form solutions are not available, numerical ones can be found. The superposition principle yields the external loading mul-

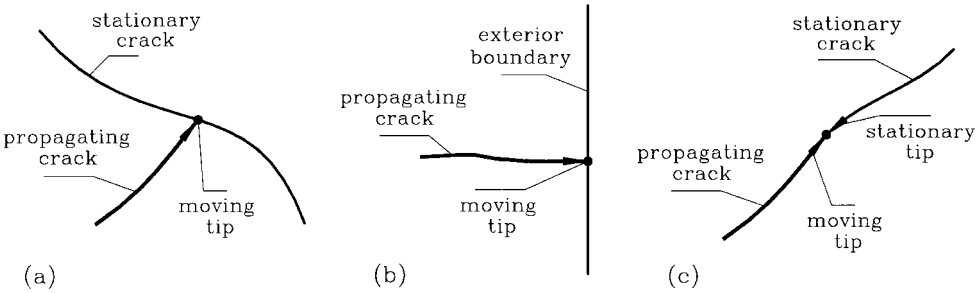

Figure 7. Crack intersection and coalescence: (a) between two cracks; (b) between a crack and the exterior boundary; (c) meeting of two tips.

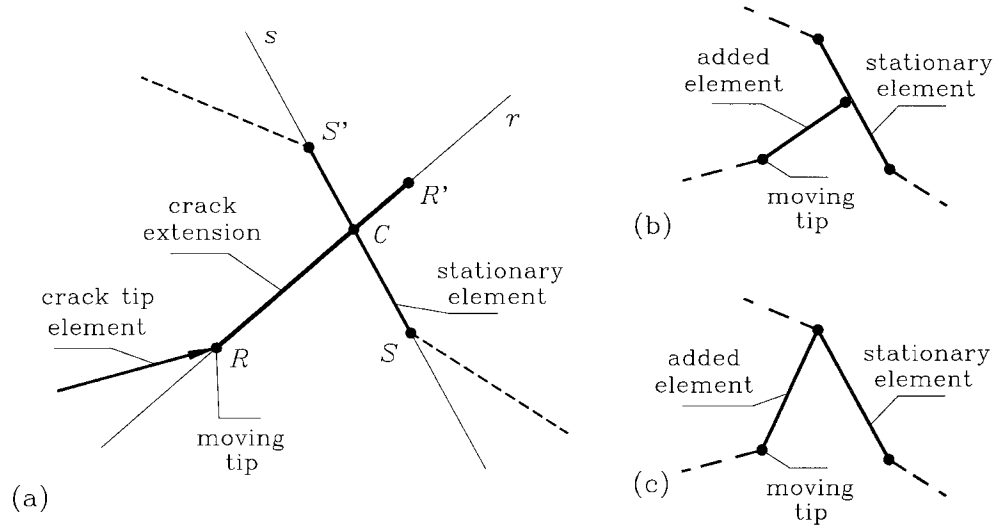

Figure 8. Intersection criterion: (a) reference notation; (b) and (c) two possible different boundary element discretizations.

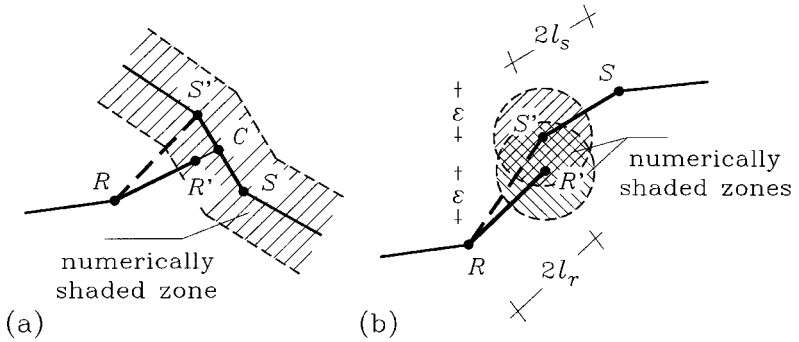

Figure 9. Zones where the numerical solution is found without sufficient accuracy: (a) along a crack line; (b) around a crack tip.

tiplier λ corresponding to the critical condition of crack growth related to the considered geometry

$$\lambda = \frac{K_{IC}}{K_{eq}}. \tag{1}$$

Incrementing the crack depth gives a new geometry which can be analysed in the same way. Failure evolution can therefore be studied simulating a loading process by means of an incremental procedure, where external load and deflection are obtained at each step by considering geometries which differ one from another in crack path.

If a multitude of cracks is considered, the length of a generic crack is not a strictly monotonic increasing function. The extension of a specific crack can be arrested because of its coalescence with a neighbouring crack or since it enters into a shielding zone. At the same time, the growth of another crack may occur. It follows that the crack controlling the fracture process can change at each step of the incremental procedure, in the sense that the crack

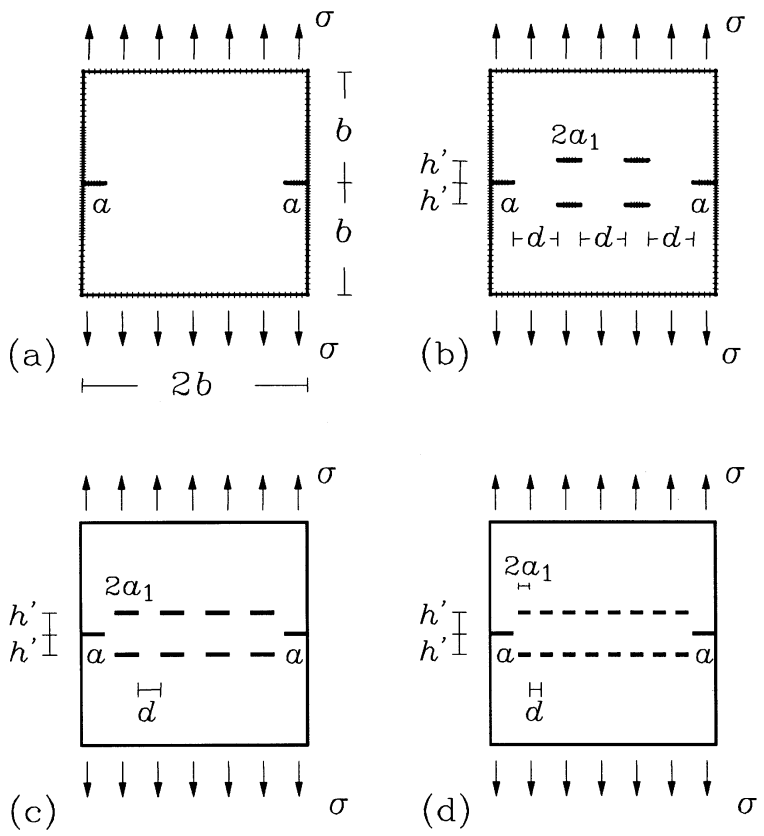

Figure 10. Square plate with interacting cracks: (a) reference geometry containing two edge cracks; comparative geometries with (b) two, (c) four and (d) eight central crack columns.

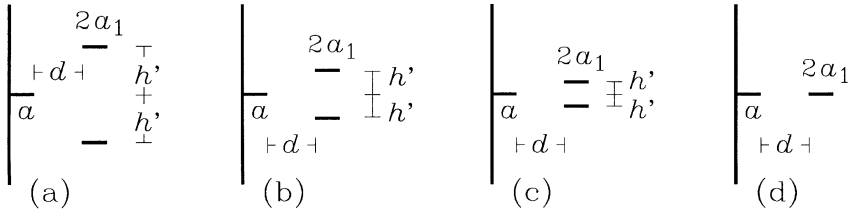

Figure 11. Comparative geometries with different vertical spacings: (a) $h'/a_1 = 4$; (b) $h'/a_1 = 2$; (c) $h'/a_1 = 1$; (d) $h'/a_1 = 0$.

length to be incremented at a specific step may be another one with respect to the preceding (Carpinteri and Monetto, 1996).

Let us consider the finite square plate with two edge cracks and two further symmetrical central cracks shown in Figure 3. The plate is in plane strain conditions and subjected to traction over the top and bottom sides. In Figure 4 the SIFs at the edge crack tips (both pointed out as A because of symmetry) are shown as functions of the relative edge crack length a/b, for three assigned values of the relative central crack length $a_1/b = 0.2$, 0.4 and 0.8. The dashed lines refer to the related SIFs at the central crack tips (each pointed out as B). The

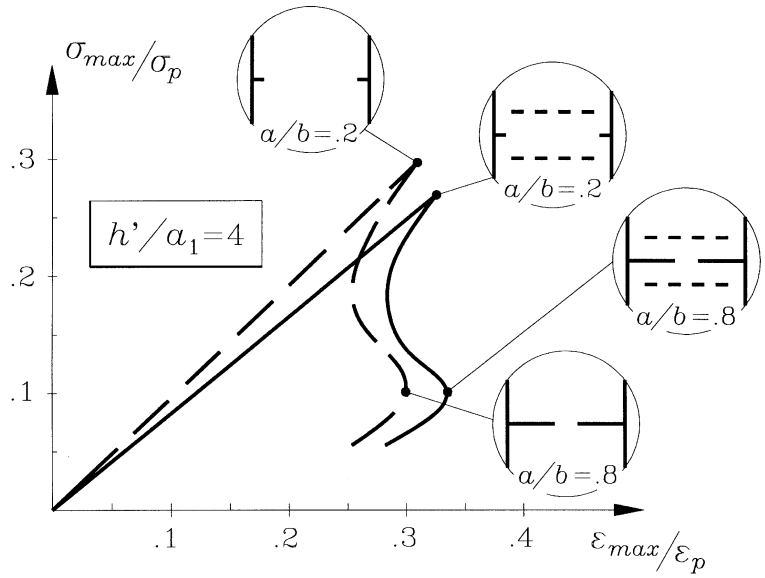

Figure 12. Normalised σ-ε diagram for eight central cracks and $h'/a_1 = 4$.

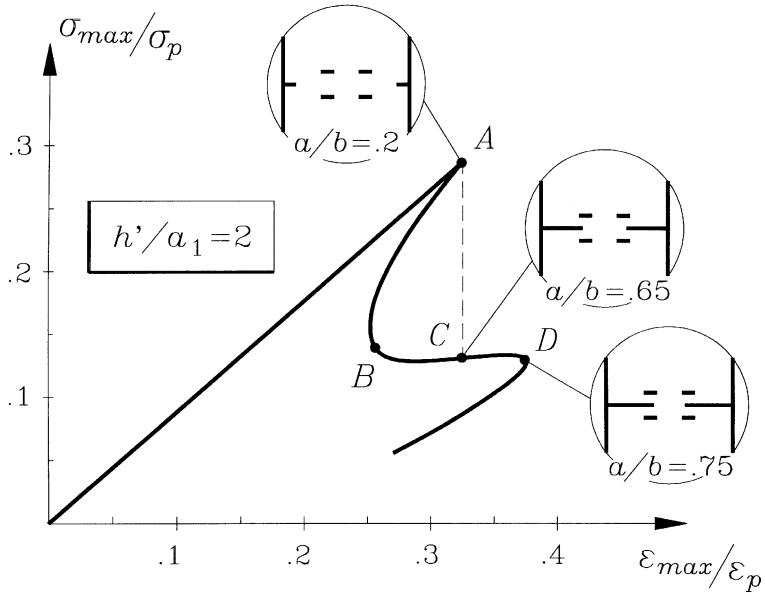

Figure 13. Normalised σ-ε diagram for four central cracks and $h'/a_1 = 2$.

SIFs are normalised through the value K_{I0} of the Mode I SIF at the tips A in the absence of the central cracks.

For $a_1/b = 0.2$ the tips A always experience the maximum SIF. It follows that the critical condition of crack propagation is first reached at such tips. The fracture evolution of the finite plate can be simulated considering a sequence of geometries which differ one from another only in the edge crack length. For longer central cracks ($a_1/b = 0.4$ and 0.8) the maximum SIF can be also experienced by the tips B. In such cases, where the dashed line is above the continuous one (shaded zones in Figure 4), the central crack length is to be incremented

to obtain the geometry corresponding to the next step of the loading process. At the points at which continuous and dashed lines cross each other, the edge cracks and the central ones interchange the role of failure controller.

In conclusion, if solids with a multitude of cracks are considered, the failure strength is associated with the imperfections which are closest to the critical condition: their length, orientation and mutual interaction induce an equivalent SIF K_{eq} at their tips which is greater than the one obtained for the other imperfections. Cracking evolution is obtained by an incremental procedure where a sequence of incremental extensions is considered, each one at those tips which experience the maximum SIF.

In other words, let be given the generic structure shown in Figure 5(a) to simulate fracture evolution induced by the assigned load distribution. At the ith step of the loading process (Figure 5(b)), the superposition principle yields the loading multiplier λ_i corresponding to the critical condition of crack growth related to the considered geometry. Equation (1) becomes

$$\lambda_i = \frac{K_{IC}}{\max(K_{\mathrm{eq}})} = \frac{K_{IC}}{K_{\mathrm{eq}}^{j}}, \tag{2}$$

experiencing the jth crack the maximum value of the equivalent SIF. Incrementing the jth crack length, the geometry to be analysed in the subsequent loading step $i + 1$ is obtained (Figure 5(c)). It is worthwhile emphasising that the crack experiencing the maximum SIF at the step $i + 1$, as well as at the step $i - 1$, can be different from the jth crack.

Unlike the quite similar algorithm developed in (Salgado and Aliabadi, 1996), only the extension of the most severely loaded crack, i.e. the one for which the greatest SIF is evaluated at its tip, is modelled. No other crack tip is assumed to reach the critical condition within the same computation step.

3. Numerical model

From a numerical point of view, simulation of fracture evolution in cracked solids and FEM have been usually combined. With reference to bi-dimensional problems, solids are represented as assemblages of finite elements which are considered to be interconnected along their boundary at specified points called nodes. In Fracture Mechanics problems the element interface along a crack line is modelled by coinciding nodes with double degree of freedom, so that crack opening and sliding displacements are allowed. According to the crack length control scheme, if the crack path is known a priori, such as in Mode I problems, double nodes can be distributed along the potential fracture line and the crack depth is incremented by untieing a node at each step. On the contrary, in Mixed Mode loading conditions, crack propagates from its tip in a direction which changes at each step. As a consequence of a crack depth increment, continuous remeshing and nodal renumbering are required. On the other hand, BEM implies that only exterior and interior boundaries, the last ones coinciding with crack faces, are discretized by a set of straight boundary elements interconnected at their ends. When a crack propagates, the subsequent geometry can be obtained by adding to the previous crack trajectory the new free surface developed in front of the moving tip. In such a way a less high computational effort is required due to the discretization of the continuum.

The basis for the proposed numerical model is the Displacement Discontinuity Boundary Element Method (DDBEM) implemented by Brencich and Carpinteri (1996) and suitably developed by the authors. The possibility of controlling the simulation through the crack

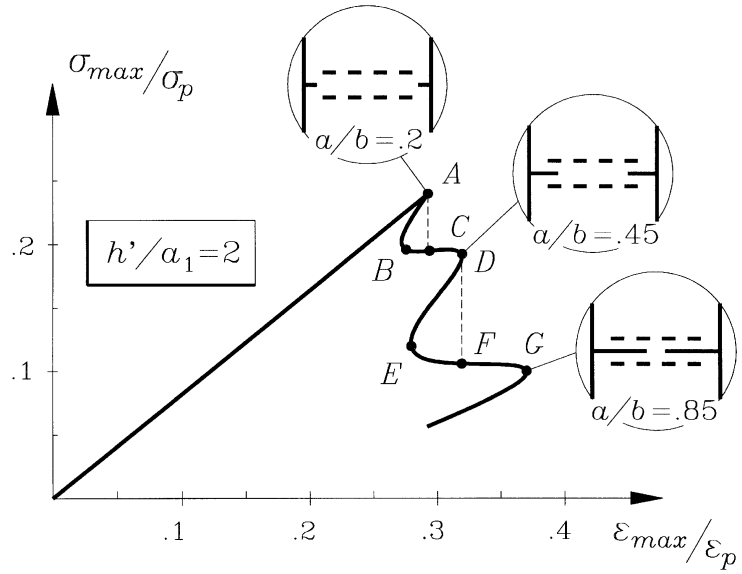

Figure 14. Normalised σ-ε diagram for eight central cracks and $h'/a_1 = 2$.

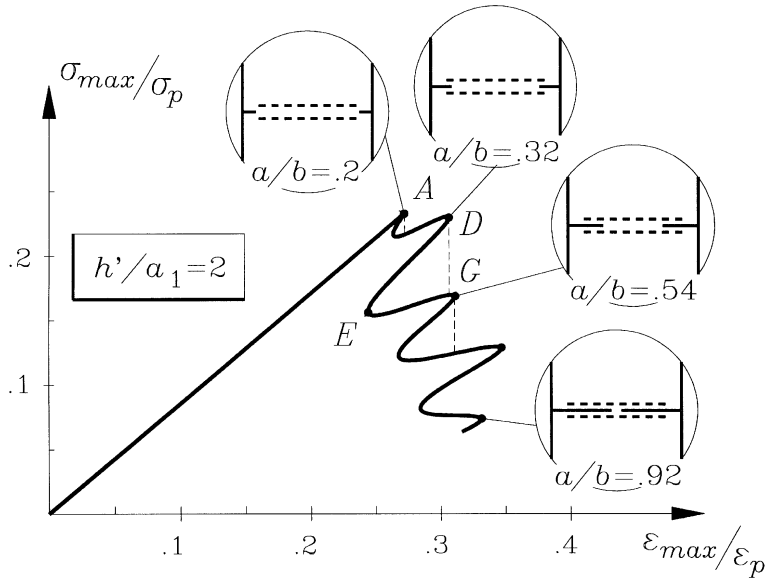

Figure 15. Normalised σ-ε diagram for sixteen central cracks and $h'/a_1 = 2$.

length has been introduced in the original algorithm. Each crack is divided into a number of straight elements over which constant displacement discontinuities are imposed in order to model the effective crack profile (Figure 6). For each element the method calculates the normal and shear displacement discontinuities D_n and D_s, which satisfy the given boundary conditions. Using D_n and D_s values, the SIFs K_{I} and K_{II} can be estimated, respectively

$$K_{\mathrm{I}} = \frac{E'}{8}\sqrt{\pi/2a}\,D_n, \tag{3a}$$

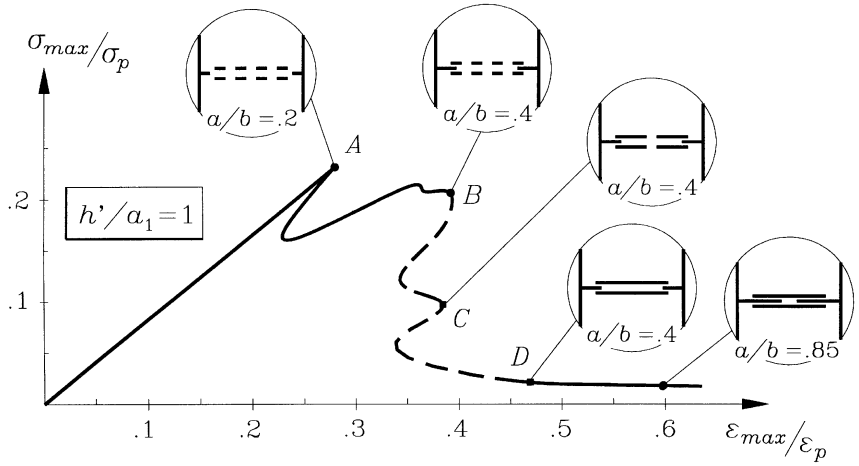

Figure 16. Normalised σ-ε diagram for eight central cracks and $h'/a_1 = 1$.

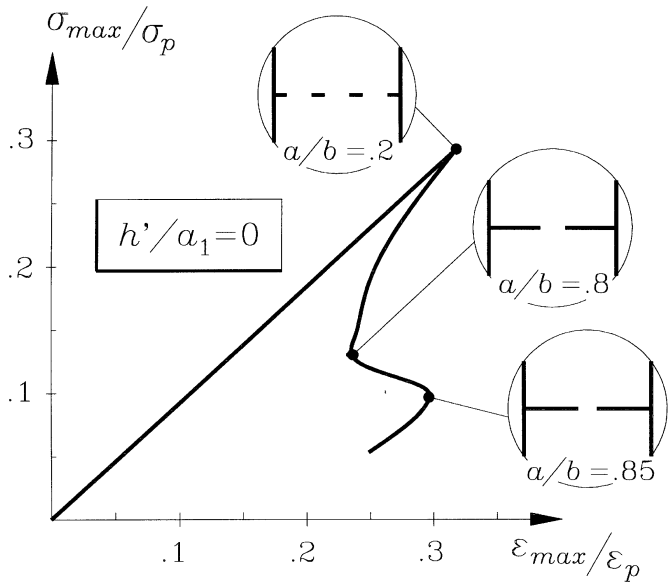

Figure 17. Normalised σ-ε diagram for two central cracks and $h'/a_1 = 0$.

$$K_{\mathrm{II}} = \frac{E'}{8}\sqrt{\pi/2a}D_s, \tag{3b}$$

where a is the semi-length of the crack tip segment; E' is a function of the Young's modulus E and of the Poisson's ratio ν of the matrix

$$E' = E, \quad \text{in plane stress,} \tag{4a}$$

$$E' = \frac{E}{1-\nu^2}, \quad \text{in plane strain.} \tag{4b}$$

With reference to those imperfections which are closest to the critical condition at a specific loading step, the Maximum Circumferential Stress Criterion (Erdogan and Sih, 1963) is used

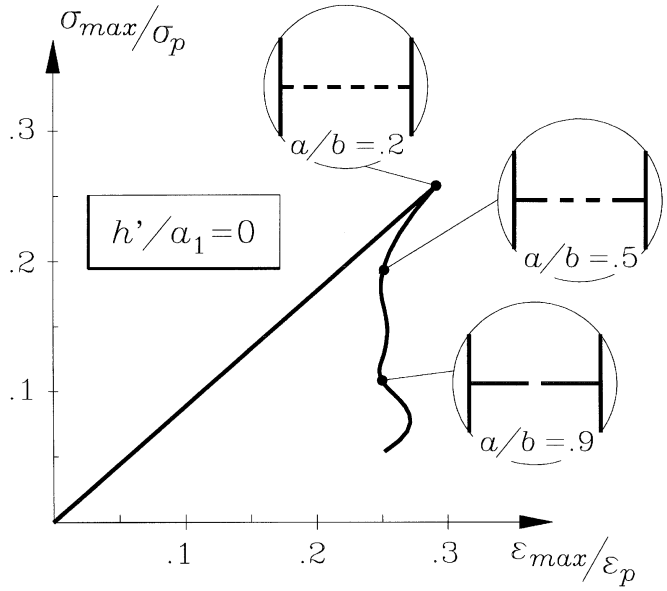

Figure 18. Normalised σ-ε diagram for four central cracks and $h'/a_1 = 0$.

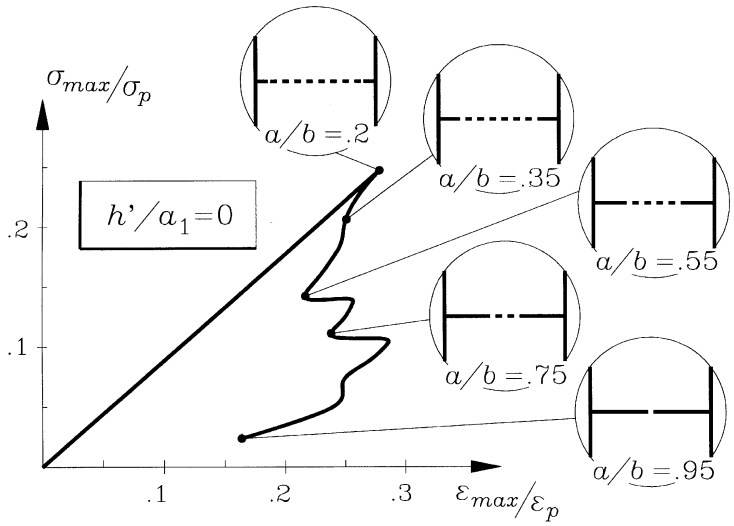

Figure 19. Normalised σ-ε diagram for eight central cracks and $h'/a_1 = 0$.

to determine the onset and the direction of crack propagation. A discrete crack extension is performed by adding a new boundary element in the direction normal to the maximum circumferential stress at the crack tip experiencing the maximum K_{eq} value. The obtained geometry refers to the subsequent loading step.

During the fracture evolution process it is possible that crack intersection occurs. A growing crack can either intersect a stationary one (Figure 7(a)) or can coalesce with it and blunt its tip (Figure 7(c)); the moving crack can also intersect the exterior boundary and become an edge crack (Figure 7(b)).

In the developed model, intersection points between each just added crack segment and all other elements are searched. With reference to Figure 8(a), let S and S' be the ends of the stationary segment, R and R' the ends of the added segment and C the related intersection point. If two segments are found to intersect, so that C belongs both to RR' and to SS' as shown in Figure 8(a), then the crack extension is terminated at the stationary element. In order to avoid not constant displacement discontinuities in SS' which would be in contrast with the definition, even though C is a generic point of SS' (Figure 8(b)), the two segments are forced to be interconnected at their ends as shown in Figure 8(c). On the other hand, analogously to the elastic equivalence principle, it can be proved that the numerical solution based on the DDBEM tends to the exact one with sufficient accuracy except at a distance from each line element equal about to its length. It follows that, even though C does not belong to RR', but the moving end R' enter the numerically shaded zone located along SS', the growing crack element is assumed to terminate against it (Figure 9(a)).

When the moving crack tip R' approaches a stationary one S', crack coalescence can occur. The problem can be conveniently discussed as an intersection problem. A zone of the continuum of extension ε all around each crack tip can be defined, where the numerical solution cannot be accepted. The extension ε is assumed to be a function of the approaching crack tip element length and is defined as follows

$$\varepsilon = \frac{l_r + l_s}{2}, \tag{5}$$

where l_r and l_s are the semi-lengths of RR' and SS', respectively. When R' enters the numerically shaded zone related to S', the crack path is rectified constraining the crack coalescence (Figure 9(b)). It is worthwhile noting that in both intersection and coalescence case rectifying crack path induces a smaller error than that of the numerical technique. In order to reduce the last one, a high number of very small boundary elements can be used such as the related shaded zones are narrow. In this way another problem can be overcome.

The Maximum Circumferential Stress Criterion (Erdogan and Sih, 1963) postulates that crack growth occurs in a direction normal to the maximum circumferential stress. The local crack growth angle ϑ^*, measured from the crack axis ahead of the tip, is determined by the condition that the local shear stress is zero

$$K_{\mathrm{I}} \sin \vartheta^* + K_{\mathrm{II}}(3 \cos \vartheta^* - 1) = 0, \tag{6}$$

which locally evaluates the tangent direction of the crack path. If a discrete crack extension increment Δa is considered, its actual direction is given by the tangent one, predicted by (6), suitably corrected by an angle β so that the propagating tip moves along the effective crack path. An iterative predictor–corrector procedure can be applied, such as that shown in (Portela et al., 1993), until a convergence condition is satisfied. If Δa tends to zero, so does the correction angle β. This means that, if very small crack extension increments are considered, (6) gives the direction of the incremental extension with sufficient accuracy modelling the continuous crack path. The iterative predictor–corrector procedure can so be avoided with a much lower computational effort. In an analysis very heavy from a numerical point of view, such as a fracture evolution simulation, it is important to come to a reasonable compromise between solution accuracy and computational time.

Table 1. Initial values of the geometric parameters defining the comparative geometries

Central crack number	a/b	a_1/b	d/b
4	0.2	0.10	0.40
8	0.2	0.10	0.16
16	0.2	0.05	0.09

4. Effects of the elastic crack interaction

The previously described numerical model is herein applied to analyse the effects of the crack interaction on the mechanical response of multi-cracked finite plates, where an initial crack distribution is contained in an elastic matrix. When the load is applied, the elastic crack interaction and the crack growth result in a global nonlinear behaviour described by more or less catastrophical softening branches of the load vs. displacement curve. The problem is discussed with reference to ordered crack distributions and plane strain loading conditions.

The reference geometry is a finite square plate with two edge cracks, subjected to traction over the top and bottom sides (Figure 10(a)). The fracture evolution is studied considering more complex geometries obtained by cutting the reference plate with two symmetrical central rows of two, four or eight evenly spaced collinear cracks (Figures 10(b,c,d)). The assumed initial relative crack lengths and ligaments for each comparative geometry are reported in Table 1.

The initial boundary element meshes are presented in Figures 10(a,b) for the reference geometry and the comparative one with two central crack columns. The exterior boundary discretization is graded towards the edge cracks with a total of two hundred segments: the boundary element size is reduced from $0.050b$, on the loaded sides, to $0.025b$, on the free sides close to the edge cracks. On the other hand, each crack is discretized with six segments of equal size, except the crack tip elements which are taken as twice the size of the contiguous ones. The crack growth increment size is assumed equal to the length of the moving crack tip element. Such a discretization criterion is the outcome of a preliminary study carried out on the reference geometry. The SIFs at the edge crack tips were evaluated varying the relative edge crack length a/b and the results compared with the approximate solution given in Rooke and Cartwright (1976). The difference does not exceed 7 percent.

Varying the relative vertical spacing h'/a_1 between the central rows and the edge cracks ($h'/a_1 = 4, 2, 1, 0$), as shown in Figure 11, the global failure behaviour is shown to be strongly dependent on the elastic crack interaction.

The greater h'/a_1, the more rapidly the influence of central cracks on the edge ones vanishes. In Figure 12 the normalised stress vs. deformation curve related to eight central cracks and $h'/a_1 = 4$ is compared with that related to the reference plate (σ_p and ε_p are, respectively, the maximum elastic stress and deformation). The brittle behaviour is characterised by a snap-back instability captured by means of the proposed method. Macroscopic fracture, qualitatively so catastrophic as for the reference geometry, is shown to be due to the unstable edge crack extension.

Decreasing h'/a_1 produces a strong influence on the global behaviour. For $h'/a_1 = 2$, the fracture evolution coincides again with the edge crack growth; nevertheless, a less catastrophic softening behaviour results. During their extension the edge cracks enter into amplification zones (branches pointed out as AB and DE in the stress vs. deformation curves of Figures 13, 14 and 15) and shielding zones (branches BD and EG in the same figures), alternately. As a consequence, the σ-ε diagrams are characterised by a series of local snap-back instabilities in a number coinciding with that of the central crack columns interacting with each edge crack tip: each instability corresponds to a single column which has a major role in the local shielding of the edge crack tip.

When the central cracks are very close to the edge cracks, the mutual interaction is so strong that the failure evolution involves both. Globally, a ductile behaviour emerges. Figure 16 shows the normalised stress vs. deformation curve related to the geometry with eight central cracks and $h'/a_1 = 1$. At first, the failure process is controlled by the edge cracks (continuous line in the diagram). The edge crack tips move and enter into the influence zone of the first central crack column. A local snap-back instability corresponds in the σ-ε curve. At the state B the central cracks reach the critical condition, grow and coalesce (dashed line), while the edge crack growth is arrested. Finally, at the state D the edge crack propagation, shielded by the central cracks, starts again. During the fracture evolution process the system assumes in all three different configurations: with eight central cracks (at the initial state pointed out as A in the diagram), with four central cracks (state C) and two (point D), as a consequence of their coalescence. Such a kind of behaviour can be proved to depend only on the relative vertical spacing value. Independently of the number of central evenly spaced columns, for $h'/a_1 = 1$ the edge and central cracks alternately propagate until the last configuration for $a/b = 0.85$ is assumed.

In the limit case, the relative vertical spacing vanishes ($h'/a_1 = 0$) and the finite plates are considered to be cut by a single row of four, six or ten collinear cracks. The related σ-ε responses are shown in Figures 17, 18 and 19, respectively. The global behaviour is brittle again and qualitatively so catastrophic as for the reference geometry (Figure 12). Macroscopic fracture is shown to be due to the extension of the edge cracks which conglobe the stationary central ones, until the plate contains only two very deep edge cracks.

In conclusion, the essential feature of the considered elastic interaction problem can be summarised by means of a comparison among the stress vs. strain curves obtained for different values of the vertical spacing. With reference to the plate cut with four central crack columns, a circular evolution of the global system ductility is evident with the perfectly brittle behaviour of the reference plate as starting and ending point. The greater the vertical spacing, the more rapidly the influence of the central cracks vanishes; the structure tends to behave as in their absence (Figure 12). When the central cracks approach the line of the edge cracks, shielding effects become stronger and the system presents a more ductile behaviour (Figures 14 and 16). On the other hand, in the limit case ($h'/a_1 = 0$) the influence is so strong that only local amplification phenomena are induced and a catastrophic brittle fracture occurs again (Figure 18).

5. Conclusions

A method of incremental loading has been developed to simulate fracture evolution of multi-cracked solids, where linear elastic homogeneous matrices contain assigned initial crack dis-

tributions. The basis of the procedure is a crack length control scheme suitably modified to account for the presence of several cracks which can interchange the role of failure controller, so that the method is successful in the analysis of snap-back problems.

Essential features of the model are:

(i) to consider a brittle crack propagation with negligible nonlinear phenomena occurring at the crack tip;
(ii) to take into account the elastic crack interaction by means of a numerical DDBEM technique;
(iii) to introduce the crack length as controlling parameter of the incremental loading process.

It follows that, at each loading step, the structure behaviour can be analysed in the framework of LEFM with reference to a unit load distribution; then the superposition principle yields the external loading multiplier corresponding to the critical condition of crack growth. A global nonlinear stress–strain behaviour is obtained resulting as a consequence of the repeated changes in the structure geometry, due to crack extensions, intersections or coalescences.

The numerical model has been successfully applied to problems involving ordered crack distributions subjected to traction. With reference to finite plates with one or more rows of evenly spaced collinear cracks, the fracture evolution has been numerically simulated and possible snap-back instabilities, each related to a local stress amplification followed by a local shielding, have been predicted. A detailed analysis of the effects of the elastic crack interaction on both fracture mechanisms and global structural response has been allowed.

Acknowledgements

The present research was carried out with the financial support of the Ministry of University and Scientific Research (MURST), the National Reasearch Council (CNR) and the EC-TMR Contract No. ERBFMRXCT960062.

References

Barpi, F. and Valente, S. (1998). Size-effects induced bifurcation during multiple cohesive crack propagation. *International Journal of Solids and Structures* **35**, 1851–1861.

Bocca, P., Carpinteri, A. and Valente, S. (1989). Fracture mechanics of brick masonry: size effects and snap-back analysis. *Materials and Structures* **22**, 364–373.

Bocca, P., Carpinteri, A. and Valente, S. (1990). Size effects in the mixed mode crack propagation: softening and snap-back analysis. *Engineering Fracture Mechanics* **35**, 159–170.

Brencich, A. and Carpinteri, A. (1996). Interaction of a main crack with ordered distributions of microcracks: a numerical technique by displacement discontinuity boundary elements. *International Journal of Fracture* **76**, 373–389.

Carpinteri, A. (1985). Interpretation of the Griffith instability as a bifurcation of the global equilibrium. *Application of Fracture Mechanics to Cementitious Composites* (Edited by S.P. Shah), Martinus Nijhoff Publishers, Dordrecht, 287–316.

Carpinteri, A. (1989). Size effects on strength, toughness and ductility. *Journal of Engineering Mechanics* **115**, 1375–1392.

Carpinteri, A. and Colombo, G. (1989). Numerical analysis of catastrophic softening behaviour (snap-back instability). *Computers and Structures* **31**, 607–636.

Carpinteri, A. and Fanelli, M. (1987). Numerical analysis of the catastrophical softening behaviour in brittle structures. *Numerical Methods in Fracture Mechanics* (Edited by A.R. Luxmoore, D.R.J. Owen, Y.P.S. Rajapakse and M.F. Kanninen), Pineridge Press, Swansea, 369–386.

Carpinteri, A. and Monetto, I. (1996). Fracture evolution and snap-back instability in multi-cracked finite plates. *Mechanisms and Mechanics of Damage and Failure* (Edited by J. Petit), Chameleon Press Ltd, London **I**, 431–436.

Carpinteri, A. and Valente, S. (1988). Numerical modelling of mixed mode cohesive crack propagation. *International Conference on Computational Engineering Science*, Atlanta, April 10–14 1988, Springer-Verlag, Berlin, 12.vi.1–2.

Carpinteri, A., Di Tommaso, A. and Fanelli, M. (1986). Influence of material parameters and geometry on cohesive crack propagation. *Fracture Toughness and Fracture Energy of Concrete* (Edited by F.H. Wittmann), Elsevier Science Publishers B.V., Amsterdam, 117–135.

Crisfield, M.A. (1981). A fast incremental/iterative solution procedure that handles 'snap-through'. *Computers and Structures* **13**, 55–62.

Erdogan, F. and Sih, G.C. (1963). On the crack extension in plates under plane loading and transverse shear. *Journal of Basic Engineering* **85**, 519–527.

Hillerborg, A., Modeer, M. and Petersson, P.E. (1976). Analysis of crack formation and crack growth in concrete by means of fracture mechanics and finite elements. *Cement and Concrete Research* **6**, 773–782.

Karman, T.V. and Tsien, H.S. (1941). The buckling of thin cylindrical shells under axial compression. *Journal of Aeronautical Science* **8**, 303–312.

Portela, A., Aliabadi, M.H. and Rooke, D.P. (1993). Dual boundary element incremental analysis of crack propagation. *Computers and Structures* **46**, 237–247.

Ramm, E. (1981). Strategies for tracing the nonlinear response near limit points. *Nonlinear Finite Element Analysis in Structural Mechanics* (Edited by W. Wunderlich, E. Stein and K.J. Bathe), Springer-Verlag, Berlin, 63–89.

Riks, E. (1979). An incremental approach to the solution of snapping and buckling problems. *International Journal of Solids and Structures* **15**, 529–551.

Rooke, D.P. and Cartwright, D.J. (1976). *Compendium of Stress Intensity Factors*, The Hillingdon Press, Uxbridge, England, 110.

Rots, J.G. and de Borst, R. (1987). Analysis of mixed-mode fracture in concrete. *Journal of Engineering Mechanics* **113**, 1739–1758; Discussion on the same paper by Carpinteri, A. and Valente, S. (1989). *Journal of Engineering Mechanics* **115**, 2344–2347.

Saleh, A.L. and Aliabadi, M.H. (1995). Crack growth analysis in concrete using boundary element method. *Engineering Fracture Mechanics* **51**, 533–545.

Salgado, N.K. and Aliabadi, M.H. (1996). The application of the dual boundary element method to the analysis of cracked stiffened panels. *Engineering Fracture Mechanics* **54**, 91–105.

Wempner, G.A. (1971). Discrete approximations related to nonlinear theories of solids. *International Journal of Solids and Structures* **7**, 1581–1599.